THE JOURNAL OF BIOLOGICAL CHEMISTRY VOL. 287, NO. 13, pp. 9982–9989, March 23, 2012

Protein Misfolding Detected Early in Pathogenesis of Transgenic Mouse Model of Huntington Disease Using Amyloid Seeding Assay*[S]

Received for publication, September 16, 2011, and in revised form, December 1, 2011 Published, JBC Papers in Press, December 20, 2011, DOI 10.1074/jbc.M111.305417

Sharad Gupta, Shy'Ann Jie, and David W. Colby[1]

From the Department of Chemical Engineering, University of Delaware, Newark, Delaware 19716

Background: Huntington disease is associated with protein misfolding.
Results: We developed an amyloid seeding assay for detecting misfolded huntingtin (HTT) protein and found early protein misfolding in a transgenic mouse model.
Conclusion: The amyloid seeding assay allows for sensitive detection of misfolded HTT.
Significance: The detection of misfolded HTT in young YAC128 mice suggests that protein misfolding may be an early event in pathogenesis.

Huntington disease (HD) is one of several fatal neurodegenerative disorders associated with misfolded proteins. Here, we report a novel method for the sensitive detection of misfolded huntingtin (HTT) isolated from the brains of transgenic (Tg) mouse models of HD and humans with HD using an amyloid seeding assay (ASA), which is based on the propensity of misfolded proteins to act as a seed and shorten the nucleation-associated lag phase in the kinetics of amyloid formation *in vitro*. Using synthetic polyglutamine peptides as the substrate for amyloid formation, we found that partially purified misfolded HTT obtained from end-stage brain tissue of two Tg HD mouse models and brain tissue of post-mortem human HD patients was capable of specifically accelerating polyglutamine amyloid formation compared with unseeded reactions and controls. Alzheimer and prion disease brain tissues did not do so, demonstrating the specificity of the ASA. It is unclear whether early intermediates or later conformational species in the protein misfolding process act as seeds in the ASA for HD. However, we were able to detect misfolded protein in the brains of YAC128 mice early in disease pathogenesis (11 weeks of age), whereas large inclusion bodies have not been observed in the brains of these mice by histology until 78 weeks of age, much later in the pathogenic process. The sensitive detection of misfolded HTT protein early in the disease pathogenesis in the YAC128 Tg mouse model strengthens the argument for a causative role of protein misfolding in HD.

Huntington disease (HD)[2] is an autosomal dominant neurodegenerative disorder characterized by progressive motor impairment, cognitive decline, and behavioral abnormalities, ultimately leading to death (1). The cause of HD is an expansion of CAG triplet repeats in exon 1 of the huntingtin (*HTT*) gene (2). One of the hallmarks of HD is the presence of a misfolded proteolytic fragment composed of the N-terminal region of huntingtin contained in neuronal intranuclear inclusions (NIIs) in post-mortem brain tissues of HD patients (3–7). Although the role of large protein agglomerates such as NIIs in the disease pathogenesis has been controversial (8–12), misfolding of the HTT protein is likely a key step in disease pathogenesis, whether at the monomeric, oligomeric, protofibril, or a later stage along the protein misfolding pathway.

Several transgenic mouse models have been developed to emulate the pathogenesis and behavioral symptoms of HD. Two of the most widely studied strains, R6/2 (13–19) and N171-82Q (20–24), exhibit NIIs early in pathogenesis. YAC128 mice express the full-length human *HTT* gene (25). They show a decline in motor control starting at 4 months, but NIIs are not seen until 18 months of age (26–29). By 12 months of age, neuronal loss can be seen in the striatum and cortex (26).

Amyloid seeding assays (ASAs), based on the propensity of misfolded proteins obtained from tissue samples to act as seeds and accelerate the *in vitro* fibrillization of monomeric protein with sequence homology (30), are a sensitive method to specifically detect the presence of misfolded proteins in prion (30) and Alzheimer (31) diseases. The kinetics of amyloid formation, as measured by thioflavin T (ThT) fluorescence (32), are so sensitive to the presence of a seed that limits of detection of a femtogram or lower have been reported (30, 33, 34). The ASA has also detected prions with atypical protease-sensitive conformations (30, 35). The real-time quaking-induced conversion ASA has been developed to quantify the amount of prions in sheep, deer, and hamsters (33) and was used to detect prions in the cerebrospinal fluid of human patients with Creutzfeldt-Jakob disease (34). Seeding recombinant HTT protein with R6/2 brain-derived seeds has been used to analyze the conformational diversity of misfolded HTT (36) but has not been investigated as a method of detection of misfolded HTT. Here, we report an ASA for sensitively detecting misfolded HTT protein

* This work was supported, in whole or in part, by National Institutes of Health Grant R00 NS064173 from NINDS and Grant P30 RR031160 from the National Center for Research Resources.
[S] This article contains supplemental Figs. 1 and 2.
[1] To whom correspondence should be addressed: Dept. of Chemical Engineering, University of Delaware, 150 Academy St., Newark, DE 19716. Tel.: 302-831-3649; E-mail: colby@udel.edu.
[2] The abbreviations used are: HD, Huntington disease; NII, neuronal intranuclear inclusion; ASA, amyloid seeding assay; ThT, thioflavin T; AD, Alzheimer disease; BTE, brain tissue equivalent; Tg, transgenic.

and then use it to demonstrate that protein misfolding occurs much earlier than previously detected in the YAC128 mouse model.

EXPERIMENTAL PROCEDURES

Peptide Solubilization—We used a modified version of a protocol reported previously (37) to create monomeric solutions of $K_2Q_{44}K_2$ (>90% purity by HPLC; Keck Biotechnology Center at Yale University). Briefly, the crude peptide was suspended in a 1:1 mixture of TFA (Acros) and hexafluoroisopropanol (ReagentWorld) at 2 mg/ml and stirred for 2 days at room temperature. Solvent was removed under argon flow, and the peptide film was dissolved in 2 M guanidine hydrochloride at 2 mg/ml. Any residual aggregates were removed by ultracentrifugation at 300,000 × *g* for 3 h at 4 °C. The top half-layer was removed and used immediately for the amyloid formation experiments.

Monitoring Amyloid Formation by ThT Assay—Disaggregated monomeric peptide was diluted with TBS (pH 8.5) and 100 μM ThT (T3516, Sigma) to an approximate peptide concentration of 0.4 mg/ml. This solution was mixed with an equal volume of seeding agent solution containing the indicated amount of preformed amyloids or partially misfolded HTT from brain tissues and transferred to 5 wells of a black 96-well flat-bottom plate (353945, BD Biosciences) containing a single 3-mm glass bead (Z143928, Sigma) for mixing. Thus, each well carried a 200-μl volume of 0.2 mg/ml peptide with 50 μM ThT and 0.2 M guanidine hydrochloride in TBS (pH 8.5) at the indicated concentration of amyloid seeds or other agents. The plate was sealed with sealing tape (235207, Fisher) and incubated in a SpectraMax M2 plate reader at 37 °C. Before each reading, the plate was shaken for 5 s, and fluorescence was recorded every 10 min with excitation at 444 nm and emission at 484 nm. Background fluorescence as recorded in the absence of peptide was subtracted from each data set. Glycogen (G0885), salmon sperm DNA (D1626), and purified brain lipid extract (B3635) were purchased from Sigma.

Transgenic Mice—All animal procedures were performed in accordance with policies set forth by the Institutional Animal Care and Use Committee at the University of Delaware. Transgenic mice (The Jackson Laboratories), including R6/2 (2810), N171-82Q (3627), and YAC128 (4938), were crossbred with the corresponding wild-type mice to create hemizygous progeny. Genotypes were confirmed by PCR according to the protocols recommended by Jackson ImmunoResearch Laboratories. R6/2 and N171-82Q mice and age-matched controls were allowed to age until they exhibited behavioral symptoms of neurodegeneration such as tremors, loss of balance, and hind limb clasping (10–14 weeks for R6/2 mice and 13–20 weeks for N171-82Q mice). Mice were killed by CO_2 asphyxiation, followed by removal of the brains. YAC128 mice and controls were killed at the ages indicated. Whole brain tissues were kept frozen at −80 °C until used.

Human Tissue Samples—Human brain tissue samples were obtained from the Harvard Brain Tissue Resource Center and the Human Brain and Spinal Fluid Resource Center at UCLA, including samples from the caudate, putamen, and acumens region of grade 4 HD-affected patients (AN 12029, 09048, 2989, and 4132) and normal non-disease donor controls (AN 08364, 16128, 3535, and 3590) and from the superior frontal cortex region of an Alzheimer disease (AD)-affected patient (AN 03349) and a normal non-disease donor control (AN 16860).

Enrichment and Partial Purification of Misfolded HTT from Brain Tissues—We modified a protocol (38) to purify misfolded HTT. Briefly, the whole brain sample from mice or the tissue block from human brain was thawed on ice and suspended in 9 volumes of homogenization buffer A (10 mM Tris, 1 mM EDTA, 0.8 M NaCl, 10% sucrose, and 0.1% Triton X-100) supplemented with protease inhibitors (1 mM PMSF (Acros) and protease inhibitor mixture (P8340, Sigma)). Tissue was homogenized on ice by extrusion through progressively thinner needles (10 passages each for 16-, 18-, and 21-gauge needles). The brain homogenate was centrifuged at 1000 × *g* for 10 min at 4 °C, and supernatant S1 was saved. The residual pellet (P1) was homogenized in 10 volumes of buffer A (with protease inhibitors) by extrusion through a 21-gauge needle. This homogenate was centrifuged at 1000 × *g* for 10 min at 4 °C, and the supernatant was mixed with S1 to yield a 5 weight % brain homogenate equivalent supernatant (S2). Four ml of S2 was adjusted to a final concentration of 1% (w/v) Sarkosyl (BP234, Fisher) and 0.2% (w/v) DTT (P-765, Boston Bioproducts) and incubated at room temperature for 2.5 h with stirring. Multimeric huntingtin and aggregates were pelleted by ultracentrifugation at 300,000 × *g* for 1.5 h at 4 °C. To remove residual Sarkosyl, pellet P3 was suspended in 4 ml of TBS and ultracentrifuged at 300,000 × *g* for 1.5 h at 4 °C. The residual pellet (P4) was suspended in TBS (pH 8.5) by stirring overnight. This suspension was passed five times through a 27-gauge needle to break up any residual large aggregates and used immediately for ThT assay. Unused seed solution was stored at −80 °C.

SDS-PAGE and Western Blotting—Pellet P4 from the protocol described for enrichment of misfolded HTT was adjusted to 2 mg of brain tissue equivalent (BTE) and visualized by Western blotting using anti-polyglutamine monoclonal antibody 1C2 (MAB1574, Millipore).

Data Analysis—To calculate the lag phase for ThT kinetic data, we identified the first of three consecutive time points that were significantly above the background and after which the signal did not fall below background. To plot the ThT fluorescence values as a function of BTE within a single assay, we calculated an average of five time point fluorescence values centered at a time point ($t_{1.25}$) that was 1.25 times the lag phase for unseeded samples. *p* values were calculated by Student's two-sample unpaired *t* test (within a single plate) or by Student's paired *t* test (for samples from different plates) using Minitab 16 software.

RESULTS

Effect of Adding Synthetic Seeds to Polyglutamine Amyloid Formation Reactions—Synthetic polyglutamine peptides, including $K_2Q_{44}K_2$, form amyloid following a lag phase upon incubation at 37 °C in buffered solution as detected by light scattering, ThT fluorescence, and sedimentation assays (39, 40). We prepared monomeric solutions of $K_2Q_{44}K_2$ using a modified version of a reported protocol (37) as follows. To delay amyloid formation in the absence of a seed, we dissolved the

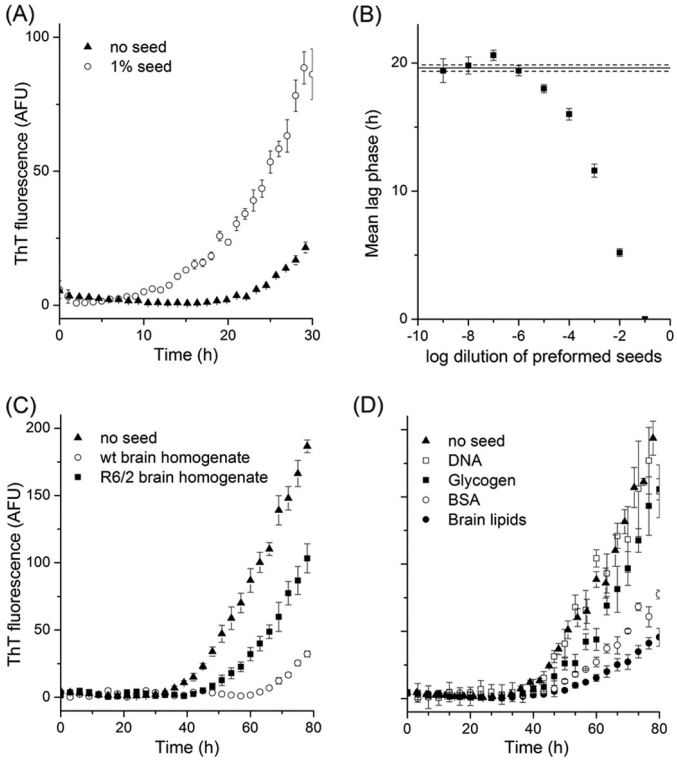

FIGURE 1. **Seeding by preformed synthetic amyloid seeds and inhibitory effect of brain homogenate on amyloid formation.** *A*, the addition of 1% preformed amyloids composed of the synthetic peptide $K_2Q_{44}K_2$ accelerated the conversion of monomeric $K_2Q_{44}K_2$ into amyloid compared with unseeded reactions as monitored by ThT fluorescence. *B*, mean lag phase (hours) for amyloid formation plotted as a function of the preformed amyloid seed concentration added to the reaction (log −1 corresponds to 10% by volume of a completed amyloid formation reaction). A significant decrease in lag phase ($p < 0.01$) was observed for a 10^{-5} dilution (or 400 pg of seed/well). *C*, the addition of brain homogenates (1% final concentrations) from both Tg R6/2 mice and WT mice inhibited amyloid formation compared with control reactions. *D*, effect of components of brain homogenate, including carbohydrates, proteins, lipids, and nucleic acids, on amyloid formation. Each *data point* represents a mean of values obtained from five wells, and *error bars* denote S.E. *AFU*, arbitrary fluorescence units.

monomeric peptide preparation in a denaturant (2 M guanidine hydrochloride) to suppress amyloid formation during subsequent processing; 2 M guanidine hydrochloride inhibited $K_2Q_{44}K_2$ amyloid formation for >4 days (data not shown). The kinetics of amyloid formation of $K_2Q_{44}K_2$ peptide in the presence and absence of preformed peptide seeds were monitored by ThT fluorescence in 96-well plates (Fig. 1, *A* and *B*). We observed a statistically significant reduction in the lag phase at seed concentrations of 0.001% (or 400 pg of preformed seed/well and higher) compared with unseeded reactions. Further dilutions resulted in no observable seeding effect.

Brain Homogenates Inhibit Amyloid Formation—We sought to examine the ability of misfolded HTT in the brains of mouse models and human brain tissues to act as seeds in amyloid formation reactions. Initially, we homogenized whole brain tissues obtained from a single end-stage R6/2 mouse and an age-matched WT control in PBS and attempted to use the crude brain homogenate to seed the amyloid formation (final concentration of 1%). We found that unpurified brain homogenates inhibited amyloid formation (Fig. 1*C*) compared with unseeded reactions. However, WT brain homogenate inhibited amyloid formation to a greater extent than R6/2 brain homogenate. We surmised that components of brain homogenate that inhibit amyloid formation may prevent sensitive detection of misfolded protein by an ASA for HD.

To determine which specific component(s) of brain homogenate inhibit amyloid formation, we added purified brain lipid extract, BSA, DNA, and glycogen individually to amyloid formation reactions. We used a physiologically relevant concentration of each biomolecule present in 1% brain homogenate. We observed that the addition of lipids (0.25 mg/ml purified brain lipid extract) and protein (0.25 mg/ml BSA) both significantly delayed amyloid formation (Fig. 1*D*). The addition of carbohydrate (0.05 mg/ml glycogen) mildly affected amyloid formation, and DNA (0.05 mg/ml) did not significantly alter the kinetics of amyloid formation (Fig. 1*D*).

Partial Purification of Misfolded HTT—Based on the observation that lipids and proteins inhibit amyloid formation, we adapted a protocol (38) to enrich misfolded HTT from brain homogenates while retaining the greatest possible yield of misfolded HTT (Fig. 2*A*). Incubation with Sarkosyl and DTT removes undesired proteins without dissolving misfolded HTT, which is largely insoluble in detergents (41). Lipids were removed by ultracentrifugation in 10% sucrose and 0.8 M NaCl. We monitored the progress of the partial purification protocol at various steps by dot blot assay (data not shown) and confirmed the presence of HTT protein in final pellet by Western blotting (Fig. 2*B*).

Sensitive Detection of Misfolded HTT in End-stage Transgenic Mouse Models and Human HD Brain Tissue by Amyloid Seeding—We subjected whole brain tissues harvested from end-stage transgenic (Tg) mouse models of HD (R6/2, $n = 3$; and N171-82Q, $n = 4$ mice), post-mortem human HD brain tissues ($n = 4$), and appropriate normal controls to the partial purification protocol. The residual pellets obtained were used to seed the conversion of $K_2Q_{44}K_2$ into amyloid.

Using 0.2 mg of BTE/well, we observed a seeding effect for all 11 samples relative to unseeded reactions and negative control samples (WT mouse and normal human brains); representative kinetic traces are shown in Fig. 3 (*A*, *C*, and *E*), longer kinetic traces are shown for 1.0 mg of BTE/well in supplemental Fig. 1. We also monitored amyloid formation as a function of the concentration of brain-derived material over 5 logs by measuring ThT fluorescence at a single time point for each sample (Fig. 3, *B*, *D*, and *F*). Samples containing misfolded HTT accelerated $K_2Q_{44}K_2$ amyloid formation at concentrations as low as 0.04 mg of BTE for R6/2 mice, 0.2 mg of BTE for N171-82Q mice, and 0.008 mg of BTE for human HD samples. We found that for all three tissue types, ThT fluorescence increased with increasing seed concentration, reached a maximum at 1 mg of BTE (Fig. 3, *B* and *D*), then decreased at higher concentrations, potentially due to remaining impurities in the samples.

To check the specificity of the HD ASA, we applied the same purification protocol to post-mortem brain obtained from an AD-affected patient and added the resulting P4 pellet to amyloid formation reactions at 1 mg of BTE. We also seeded the amyloid formation reaction with 1 mg of BTE of scrapie prion that was partially purified by phosphotungstic acid precipitation (30) from RML/Chandler-infected FVB mouse brain tissue

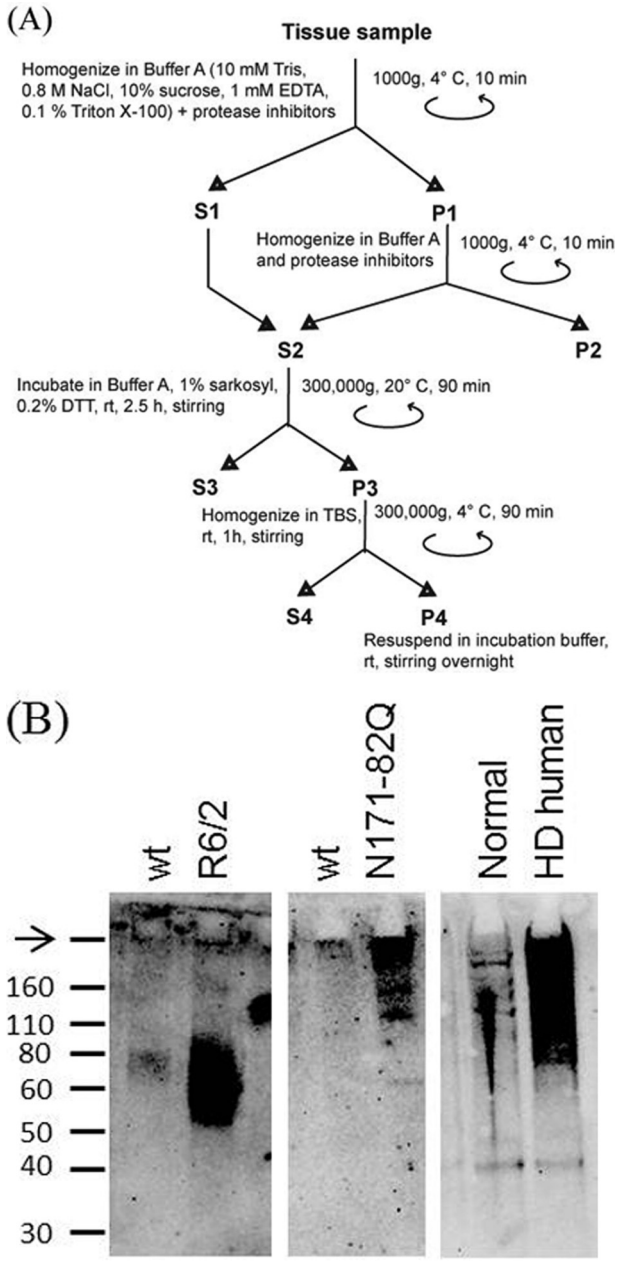

FIGURE 2. **Partial purification of misfolded HTT from brain tissue homogenate.** *A*, schematic of the purification protocol used (modified from Ref. 38). The resulting pellet (P4) was used in subsequent seeding experiments. *B*, the presence of HTT in pellet P4 was confirmed by Western blotting with antibody 1C2. Misfolded HTT protein from Tg N171-82Q mice and human HD tissue barely penetrated the gel, whereas that from Tg R6/2 mice appeared to be soluble in boiling SDS. The *arrow* denotes the well position.

samples. In both cases, amyloid formation was comparable with negative controls (Fig. 3*G*).

Statistical Confidence in HD ASA for Detecting Misfolded HTT Protein—The preceding analyses using human HD samples, as well as R6/2 and N171-82Q mouse samples, were all performed on end-stage samples containing misfolded HTT. To check the combined statistical significance of all of the measurements made using the HD ASA, we plotted the mean value of ThT fluorescence observed for 1 mg of BTE for each of the tissue samples analyzed ($n = 11$ samples containing misfolded HTT and $n = 15$ negative controls) (Fig. 4). To analyze the data on a single scale, we used a time point ($t_{1.25}$) that was 1.25 times the lag phase for unseeded samples. This analysis indicated that the HD ASA can detect the presence of misfolded HTT with a high degree of statistical confidence ($p < 0.001$).

Detection of Misfolded HTT in 11-week-old YAC128 Mice—Having establishing that the ASA can detect the presence of misfolded HTT in partially purified brain tissue samples from end-stage HD mouse models and post-mortem human HD samples, we next examined whether the ASA can detect misfolded HTT in an age-dependent manner in YAC128 mice, in which misfolded protein is not seen until 18 months of age (26–28). We subjected whole brain tissue harvested from YAC128 mice at different ages (3.4 ($n = 1$), 7.4 ($n = 3$), 11 ($n = 1$), 12 ($n = 3$), 21 ($n = 2$), and 33 ($n = 1$) weeks) and age-matched WT controls to the partial purification protocol and added the resulting P4 pellets to amyloid formation reactions (Fig. 5 and supplemental Fig. 2).

Amyloid seeding was observed in an age- and dose-dependent manner. Although an increase in ThT fluorescence could be seen after the addition of 5 mg of BTE of the P4 fraction derived from mice 12 weeks and older (Fig. 5, *A* and *B*), age dependence was more evident at 1 mg of BTE (Fig. 5, *C* and *D*). We also determined the dose dependence of amyloid seeding over a broader range for YAC128 mice 3.4, 7.4, 11, 12, 21, and 33 weeks of age (Fig. 5, *E*–*G*). To investigate the possibility that this age dependence is merely a manifestation of increasing expression levels of the transgene for HTT as the mice age, we measured HTT protein levels in YAC128 mice for the range of time points used and established that there was no change in expression levels with age (data not shown).

DISCUSSION

We have developed a sensitive ASA for the detection of misfolded HTT in brain tissues from HD mouse models and humans with HD and have demonstrated that the ASA can detect the misfolding of HTT in the YAC128 mouse model much earlier than demonstrated with other methods (26). The short synthetic peptide $K_2Q_{44}K_2$ was chosen as the substrate for ASA because it is available commercially and has well characterized amyloid formation kinetics (37, 39, 40). Reaction conditions were identified that resulted in a well defined lag phase (>20 h) (Fig. 1*A*), allowing for observation of a seeding effect with as little as 400 pg of preformed $K_2Q_{44}K_2$ amyloid. Presumably further optimization of the conditions used for the HD ASA could result in greater sensitivity or a more facile assay, as was demonstrated by altering the conditions used for the original prion ASA (30, 33).

Material recovered from WT samples during the purification protocol resulted in slightly higher ThT fluorescence values when added to amyloid formation reactions compared with unseeded reactions (*e.g.* Fig. 3*A*). We attribute this to trace compounds either from brain homogenate or from chemicals used in the purification procedure that may be retained in the final pellet upon ultracentrifugation.

Upon seeding amyloid formation reactions with misfolded HTT isolated from HD mouse models, we observed a nonlinear dependence of the amount of seed added on the increase in ThT fluorescence (*e.g.* Fig. 3*B*). This may have been due to the cumulative effect of two opposing factors: an

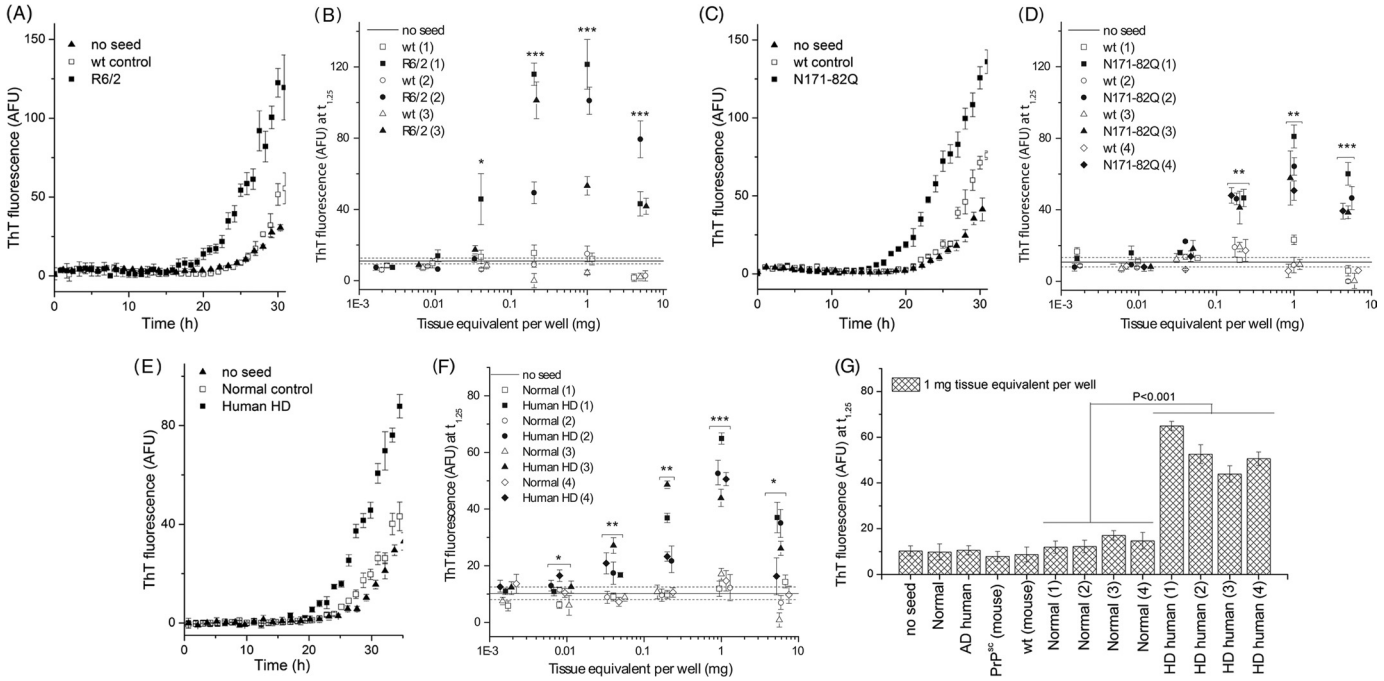

FIGURE 3. **Misfolded HTT, purified from brains of Tg HD mouse models and humans with HD, accelerates conversion of monomeric $K_2Q_{44}K_2$ into amyloid.** *A*, *C*, and *E*, typical amyloid formation kinetics following the addition of 0.2 mg of tissue equivalent/well of the P4 fraction recovered from R6/2 mice, N171-82Q mice, and human HD samples. *B*, *D*, and *F*, acceleration of amyloid formation was dependent upon the amount of misfolded HTT added as estimated by measuring the ThT fluorescence at time point $t_{1.25}$ (defined in under "Experimental Procedures"). *G*, the HD ASA specifically detected misfolded HTT, and not misfolded protein found in human AD disease brain, such as amyloid-β plaques or tau tangles, subjected to the same purification protocol. The addition of partially purified PrP^{Sc} from prion-infected mouse brain by phosphotungstic acid precipitation did not accelerate amyloid formation in the HD ASA. Data shown are for 1 mg of tissue equivalent/well. *p* values were calculated using Student's paired *t* test on data collected from independent samples. *Symbol shape* denotes paired samples. *, $p < 0.05$; **, $p < 0.01$; ***, $p < 0.001$. Each *data point* represents the mean values of four to five wells, and *error bars* denote S.E. obtained for a single brain sample. *AFU*, arbitrary fluorescence units.

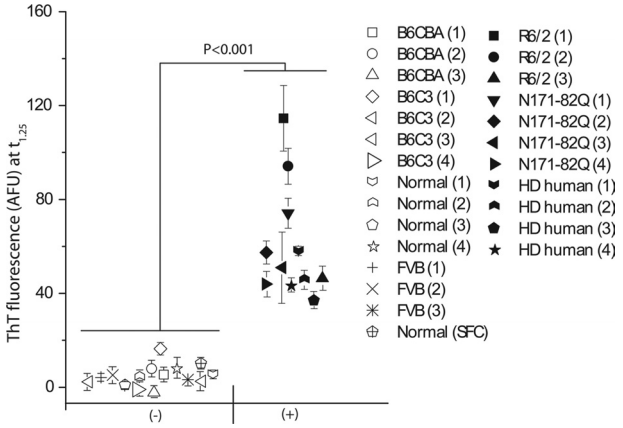

FIGURE 4. **Statistical confidence in HD ASA for detection of misfolded HTT protein.** We compared the ThT fluorescence values obtained in the ASA for samples known to contain misfolded HTT ($n = 11$) with the values for samples from wild-type animals and humans without HD ($n = 15$). For each tissue sample, the mean ThT fluorescence value observed in 5 wells at $t_{1.25}$ is shown. *Closed symbols* represent HD-positive samples, and *open symbols* represent corresponding WT or non-disease samples. *Error bars* denote S.E. *AFU*, arbitrary fluorescence units.

increase in misfolded HTT seed concentration, which accelerates amyloid formation, is accompanied by an increase in cellular contaminants (such as membrane bound lipids and proteins) that co-pellet with misfolded HTT and tend to inhibit amyloid formation.

The limit of detection for partially purified misfolded HTT in HD ASA is ~40 μg of BTE for mouse models (R6/2 and N171-82Q) (Fig. 3, *B* and *D*), on the same order as reported for the AD ASA (40 μg of BTE) (31) but significantly lower than that observed for the prion ASA (3.4 ng of BTE after phosphotungstic acid precipitation) (30). It is likely that the sensitivity of each assay depends both on the relative concentration of misfolded protein in brain tissues in each disease and on the amyloidogenicity of each misfolded protein.

One could argue that the misfolded protein that we detected was formed during the purification process. However, two observations argue against this hypothesis. First, no acceleration in amyloid formation was observed for the 7.4-week-old YAC128 mouse even though the protein levels at this age are the same as those observed in older YAC128 mice. Second, there was a clear age dependence on the magnitude of the increase in ThT fluorescence observed following seeding with material isolated from the YAC128 mice, implying that the misfolded protein content increases over the age range investigated. If the amyloid seeding effect was an artifact of the purification protocol, no such trend would be observed.

There is no direct correlation between the presence of NIIs and neurotoxicity: in some mouse models such as R6/2 (14) and N171-82Q (42), NIIs precede onset of HD-related behavioral symptoms, whereas in other mouse models such as YAC128 (26, 43) and knock-in models (44, 45), NIIs are not visible until late stages of the disease. In the YAC128 model, motor impairment has been observed by 4 months (27), with nuclear immunostaining of HTT seen as early as 2 months, although NIIs are

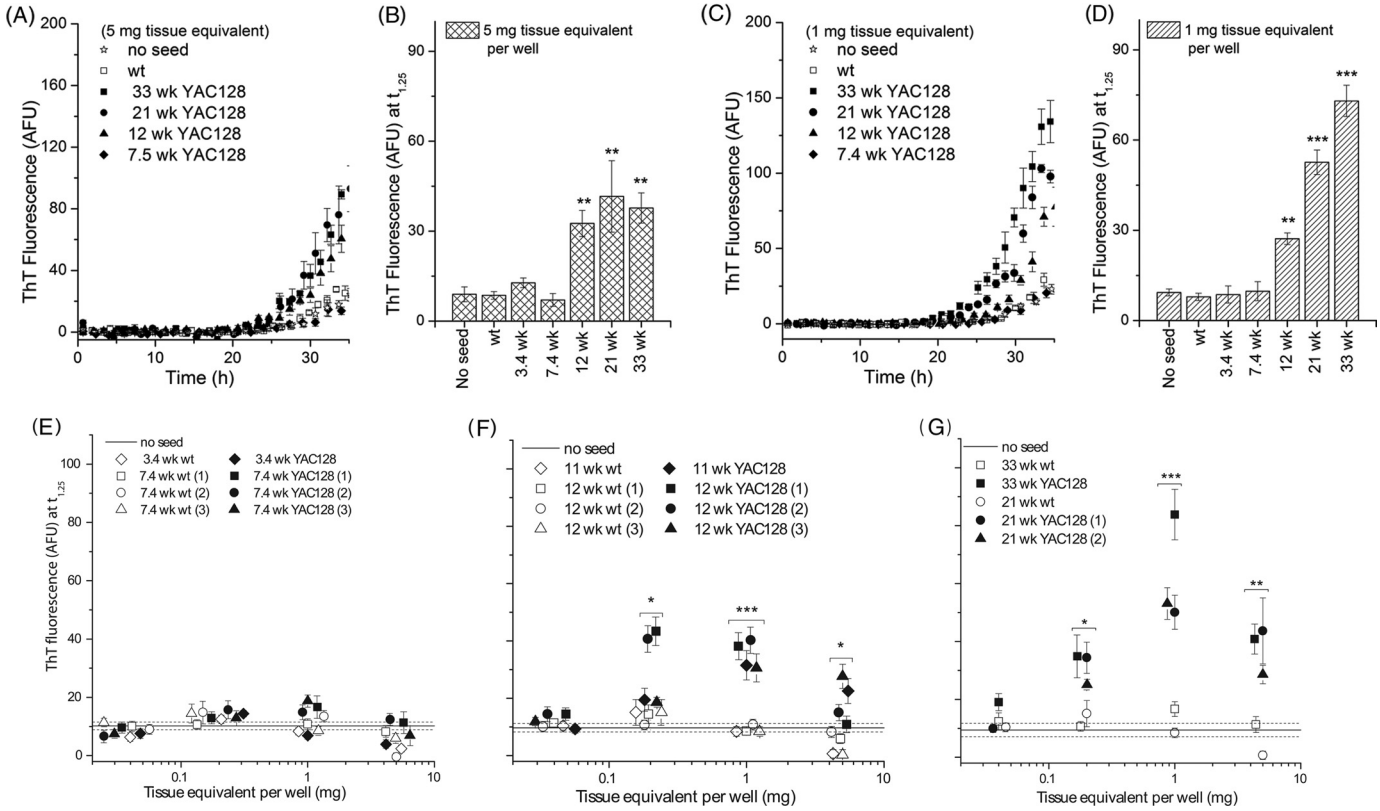

FIGURE 5. **HD ASA detects presence of misfolded HTT in YAC128 mouse brain tissue as early as 11 weeks of age.** *A* and *C*, representative kinetics of amyloid formation in the presence of partially purified misfolded HTT obtained from YAC128 mice at the ages indicated for 5 and 1 mg of tissue equivalent/well. *B* and *D*, acceleration in amyloid formation as a function of age as estimated by ThT fluorescence at 1.25 for 5 and 1 mg of tissue equivalent/well. *E–G*, ThT fluorescence at $t_{1.25}$ as a function of seed concentration/well for YAC128 mice at the ages indicated. In *E–G*, overlapping ThT fluorescence values are offset slightly horizontally for clarity. *p* values were calculated using Student's paired *t* test on results from independent brain samples. *Symbol shape* denotes paired samples. *, $p < 0.05$; **, $p < 0.01$; ***, $p < 0.001$. Each *data point* represents a mean of values obtained from four to five wells, and *error bars* denote S.E. for a single brain sample. *AFU*, arbitrary fluorescence units.

not visible until 18 months of age (26). We do not know if the HD ASA detects large NIIs or earlier intermediates in the protein misfolding process, such as oligomers (46). However, we have demonstrated that some form of misfolded HTT can be detected by 11 weeks of age. Thus, HTT misfolding takes place early in the pathogenesis of disease in the YAC128 model and can be observed around the same time that the earliest behavioral symptoms begin to manifest (27), consistent with the observation in cell culture experiments that misfolded HTT nucleation occurs randomly in time (47). It is possible that, because of their small size, these intermediates are not visible by immunostaining or that NIIs are present at early ages but not at sufficient densities to easily detect by neuropathology, which typically entails examining slices that compose only a small volume of the brain.

The sensitivity of the HD ASA and its ability to detect misfolded HTT early may make the assay useful as a biomarker for HD pathogenesis in preclinical trials, especially in studies aimed at determining the effectiveness of putative HD therapeutics in the YAC128 mouse model. Our findings also suggest that drugs directed toward preventing protein misfolding (*e.g.* Ref. 48) should be administered early in this mouse model. If the HD ASA can be extended to the detection of misfolded HTT in peripheral tissues or blood of HD patients, it may be a useful biomarker for clinical trials as well.

Acknowledgments—We thank Natalie Barnes for help with breeding mouse colonies and harvesting tissue samples, Zachary March for purification of AD and control brain tissue samples, and Kyle Doolan for purification of PrP^{Sc} from brain tissue sample. We thank the patients and families who donated tissue samples and the Harvard Brain Tissue Resource Center (supported in part by United States Public Health Service Grant R24 MH068855 from the National Institutes of Health) and the Human Brain and Spinal Fluid Resource Center at UCLA (supported in part by NINDS/National Institute of Mental Health) for providing tissues.

REFERENCES

1. Huntington, G. (1872) On chorea. *Med. Surg. Rep.* **26,** 317–321
2. The Huntington Disease Collaborative Research Group (1993) A novel gene containing a trinucleotide repeat that is expanded and unstable on Huntington disease chromosomes. *Cell* **72,** 971–983
3. DiFiglia, M., Sapp, E., Chase, K. O., Davies, S. W., Bates, G. P., Vonsattel, J. P., and Aronin, N. (1997) Aggregation of huntingtin in neuronal intranuclear inclusions and dystrophic neurites in brain. *Science* **277,** 1990–1993
4. Gourfinkel-An, I., Cancel, G., Duyckaerts, C., Faucheux, B., Hauw, J. J., Trottier, Y., Brice, A., Agid, Y., and Hirsch, E. C. (1998) Neuronal distribution of intranuclear inclusions in Huntington disease with adult onset. *Neuroreport* **9,** 1823–1826
5. Herndon, E. S., Hladik, C. L., Shang, P., Burns, D. K., Raisanen, J., and White, C. L. (2009) Neuroanatomic profile of polyglutamine immunoreactivity in Huntington disease brains. *J. Neuropathol. Exp. Neurol.* **68,**

250–261
6. Maat-Schieman, M., Roos, R., Losekoot, M., Dorsman, J., Welling-Graafland, C., Hegeman-Kleinn, I., Broeyer, F., Breuning, M., and van Duinen, S. (2007) Neuronal intranuclear and neuropil inclusions for pathological assessment of Huntington disease. *Brain Pathol.* **17,** 31–37
7. Sieradzan, K. A., Mechan, A. O., Jones, L., Wanker, E. E., Nukina, N., and Mann, D. M. (1999) Huntington disease intranuclear inclusions contain truncated, ubiquitinated huntingtin protein. *Exp. Neurol.* **156,** 92–99
8. Saudou, F., Finkbeiner, S., Devys, D., and Greenberg, M. E. (1998) Huntingtin acts in the nucleus to induce apoptosis, but death does not correlate with the formation of intranuclear inclusions. *Cell* **95,** 55–66
9. Arrasate, M., Mitra, S., Schweitzer, E. S., Segal, M. R., and Finkbeiner, S. (2004) Inclusion body formation reduces levels of mutant huntingtin and the risk of neuronal death. *Nature* **431,** 805–810
10. Yang, W., Dunlap, J. R., Andrews, R. B., and Wetzel, R. (2002) Aggregated polyglutamine peptides delivered to nuclei are toxic to mammalian cells. *Hum. Mol. Genet.* **11,** 2905–2917
11. Campioni, S., Mannini, B., Zampagni, M., Pensalfini, A., Parrini, C., Evangelisti, E., Relini, A., Stefani, M., Dobson, C. M., Cecchi, C., and Chiti, F. (2010) A causative link between the structure of aberrant protein oligomers and their toxicity. *Nat. Chem. Biol.* **6,** 140–147
12. Nucifora, F. C., Jr., Sasaki, M., Peters, M. F., Huang, H., Cooper, J. K., Yamada, M., Takahashi, H., Tsuji, S., Troncoso, J., Dawson, V. L., Dawson, T. M., and Ross, C. A. (2001) Interference by huntingtin and atrophin-1 with CBP-mediated transcription leading to cellular toxicity. *Science* **291,** 2423–2428
13. Mangiarini, L., Sathasivam, K., Seller, M., Cozens, B., Harper, A., Hetherington, C., Lawton, M., Trottier, Y., Lehrach, H., Davies, S. W., and Bates, G. P. (1996) Exon 1 of the HD gene with an expanded CAG repeat is sufficient to cause a progressive neurological phenotype in transgenic mice. *Cell* **87,** 493–506
14. Davies, S. W., Turmaine, M., Cozens, B. A., DiFiglia, M., Sharp, A. H., Ross, C. A., Scherzinger, E., Wanker, E. E., Mangiarini, L., and Bates, G. P. (1997) Formation of neuronal intranuclear inclusions underlies the neurological dysfunction in mice transgenic for the HD mutation. *Cell* **90,** 537–548
15. Dedeoglu, A., Kubilus, J. K., Jeitner, T. M., Matson, S. A., Bogdanov, M., Kowall, N. W., Matson, W. R., Cooper, A. J., Ratan, R. R., Beal, M. F., Hersch, S. M., and Ferrante, R. J. (2002) Therapeutic effects of cystamine in a murine model of Huntington disease. *J. Neurosci.* **22,** 8942–8950
16. DeMarch, Z., Giampà, C., Patassini, S., Bernardi, G., and Fusco, F. R. (2008) Beneficial effects of rolipram in the R6/2 mouse model of Huntington disease. *Neurobiol. Dis.* **30,** 375–387
17. Ferrante, R. J., Andreassen, O. A., Jenkins, B. G., Dedeoglu, A., Kuemmerle, S., Kubilus, J. K., Kaddurah-Daouk, R., Hersch, S. M., and Beal, M. F. (2000) Neuroprotective effects of creatine in a transgenic mouse model of Huntington disease. *J. Neurosci.* **20,** 4389–4397
18. Li, H., Li, S. H., Cheng, A. L., Mangiarini, L., Bates, G. P., and Li, X. J. (1999) Ultrastructural localization and progressive formation of neuropil aggregates in Huntington disease transgenic mice. *Hum. Mol. Genet.* **8,** 1227–1236
19. Simmons, D. A., Mehta, R. A., Lauterborn, J. C., Gall, C. M., and Lynch, G. (2011) Brief ampakine treatments slow the progression of Huntington disease phenotypes in R6/2 mice. *Neurobiol. Dis.* **41,** 436–444
20. Schilling, G., Becher, M. W., Sharp, A. H., Jinnah, H. A., Duan, K., Kotzuk, J. A., Slunt, H. H., Ratovitski, T., Cooper, J. K., Jenkins, N. A., Copeland, N. G., Price, D. L., Ross, C. A., and Borchelt, D. R. (1999) Intranuclear inclusions and neuritic aggregates in transgenic mice expressing a mutant N-terminal fragment of huntingtin. *Hum. Mol. Genet.* **8,** 397–407
21. Andreassen, O. A., Dedeoglu, A., Ferrante, R. J., Jenkins, B. G., Ferrante, K. L., Thomas, M., Friedlich, A., Browne, S. E., Schilling, G., Borchelt, D. R., Hersch, S. M., Ross, C. A., and Beal, M. F. (2001) Creatine increases survival and delays motor symptoms in a transgenic animal model of Huntington disease. *Neurobiol. Dis.* **8,** 479–491
22. Harper, S. Q., Staber, P. D., He, X., Eliason, S. L., Martins, I. H., Mao, Q., Yang, L., Kotin, R. M., Paulson, H. L., and Davidson, B. L. (2005) RNA interference improves motor and neuropathological abnormalities in a Huntington disease mouse model. *Proc. Natl. Acad. Sci. U.S.A.* **102,** 5820–5825
23. Masuda, N., Peng, Q., Li, Q., Jiang, M., Liang, Y., Wang, X., Zhao, M., Wang, W., Ross, C. A., and Duan, W. (2008) Tiagabine is neuroprotective in the N171-82Q and R6/2 mouse models of Huntington disease. *Neurobiol. Dis.* **30,** 293–302
24. Zádori, D., Nyiri, G., Szonyi, A., Szatmári, I., Fülöp, F., Toldi, J., Freund, T. F., Vécsei, L., and Klivényi, P. (2011) Neuroprotective effects of a novel kynurenic acid analogue in a transgenic mouse model of Huntington disease. *J. Neural Transm.* **118,** 865–875
25. Hodgson, J. G., Agopyan, N., Gutekunst, C. A., Leavitt, B. R., LePiane, F., Singaraja, R., Smith, D. J., Bissada, N., McCutcheon, K., Nasir, J., Jamot, L., Li, X. J., Stevens, M. E., Rosemond, E., Roder, J. C., Phillips, A. G., Rubin, E. M., Hersch, S. M., and Hayden, M. R. (1999) A YAC mouse model for Huntington disease with full-length mutant huntingtin, cytoplasmic toxicity, and selective striatal neurodegeneration. *Neuron* **23,** 181–192
26. Slow, E. J., van Raamsdonk, J., Rogers, D., Coleman, S. H., Graham, R. K., Deng, Y., Oh, R., Bissada, N., Hossain, S. M., Yang, Y. Z., Li, X. J., Simpson, E. M., Gutekunst, C. A., Leavitt, B. R., and Hayden, M. R. (2003) Selective striatal neuronal loss in a YAC128 mouse model of Huntington disease. *Hum. Mol. Genet.* **12,** 1555–1567
27. Van Raamsdonk, J. M., Pearson, J., Slow, E. J., Hossain, S. M., Leavitt, B. R., and Hayden, M. R. (2005) Cognitive dysfunction precedes neuropathology and motor abnormalities in the YAC128 mouse model of Huntington disease. *J. Neurosci.* **25,** 4169–4180
28. Crook, Z. R., and Housman, D. (2011) Huntington's disease: can mice lead the way to treatment? *Neuron* **69,** 423–435
29. Van Raamsdonk, J. M., Metzler, M., Slow, E., Pearson, J., Schwab, C., Carroll, J., Graham, R. K., Leavitt, B. R., and Hayden, M. R. (2007) Phenotypic abnormalities in the YAC128 mouse model of Huntington disease are penetrant on multiple genetic backgrounds and modulated by strain. *Neurobiol. Dis.* **26,** 189–200
30. Colby, D. W., Zhang, Q., Wang, S., Groth, D., Legname, G., Riesner, D., and Prusiner, S. B. (2007) Prion detection by an amyloid seeding assay. *Proc. Natl. Acad. Sci. U.S.A.* **104,** 20914–20919
31. Du, D., Murray, A. N., Cohen, E., Kim, H. E., Simkovsky, R., Dillin, A., and Kelly, J. W. (2011) A kinetic aggregation assay allowing selective and sensitive amyloid-β quantification in cells and tissues. *Biochemistry* **50,** 1607–1617
32. Saeed, S. M., and Fine, G. (1967) Thioflavin T for amyloid detection. *Am. J. Clin. Pathol.* **47,** 588–593
33. Wilham, J. M., Orru, C. D., Bessen, R. A., Atarashi, R., Sano, K., Race, B., Meade-White, K. D., Taubner, L. M., Timmes, A., and Caughey, B. (2010) Rapid end-point quantitation of prion seeding activity with sensitivity comparable to bioassays. *PLoS Pathog.* e1001217
34. Atarashi, R., Satoh, K., Sano, K., Fuse, T., Yamaguchi, N., Ishibashi, D., Matsubara, T., Nakagaki, T., Yamanaka, H., Shirabe, S., Yamada, M., Mizusawa, H., Kitamoto, T., Klug, G., McGlade, A., Collins, S. J., and Nishida, N. (2011) Ultrasensitive human prion detection in cerebrospinal fluid by real-time quaking-induced conversion. *Nat. Med.* **17,** 175–178
35. Colby, D. W., Wain, R., Baskakov, I. V., Legname, G., Palmer, C. G., Nguyen, H. O. B., Lemus, A., Cohen, F. E., DeArmond, S. J., and Prusiner, S. B. (2010) Protease-sensitive synthetic prions. *PLoS Pathog.* e1000736
36. Nekooki-Machida, Y., Kurosawa, M., Nukina, N., Ito, K., Oda, T., and Tanaka, M. (2009) Distinct conformations of *in vitro* and *in vivo* amyloids of huntingtin exon 1 show different cytotoxicity. *Proc. Natl. Acad. Sci. U.S.A.* **106,** 9679–9684
37. O'Nuallain, B., Thakur, A. K., Williams, A. D., Bhattacharyya, A. M., Chen, S., Thiagarajan, G., and Wetzel, R. (2006) Kinetics and thermodynamics of amyloid assembly using a high-performance liquid chromatography-based sedimentation assay. *Methods Enzymol.* **413,** 34–74
38. Díaz-Hernández, M., Moreno-Herrero, F., Gómez-Ramos, P., Morán, M. A., Ferrer, I., Baró, A. M., Avila, J., Hernández, F., and Lucas, J. J. (2004) Biochemical, ultrastructural, and reversibility studies on huntingtin filaments isolated from mouse and human brain. *J. Neurosci.* **24,** 9361–9371
39. Chen, S., Berthelier, V., Yang, W., and Wetzel, R. (2001) Polyglutamine aggregation behavior *in vitro* supports a recruitment mechanism of cytotoxicity. *J. Mol. Biol.* **311,** 173–182
40. Chen, S., Ferrone, F. A., and Wetzel, R. (2002) Huntington disease age of onset linked to polyglutamine aggregation nucleation. *Proc. Natl. Acad.*

Sci. U.S.A. **99,** 11884–11889
41. Scherzinger, E., Lurz, R., Turmaine, M., Mangiarini, L., Hollenbach, B., Hasenbank, R., Bates, G. P., Davies, S. W., Lehrach, H., and Wanker, E. E. (1997) Huntingtin-encoded polyglutamine expansions form amyloid-like protein aggregates *in vitro* and *in vivo*. *Cell* **90,** 549–558
42. Schilling, G., Jinnah, H. A., Gonzales, V., Coonfield, M. L., Kim, Y., Wood, J. D., Price, D. L., Li, X. J., Jenkins, N., Copeland, N., Moran, T., Ross, C. A., and Borchelt, D. R. (2001) Distinct behavioral and neuropathological abnormalities in transgenic mouse models of HD and DRPLA. *Neurobiol. Dis.* **8,** 405–418
43. Van Raamsdonk, J. M., Murphy, Z., Slow, E. J., Leavitt, B. R., and Hayden, M. R. (2005) Selective degeneration and nuclear localization of mutant huntingtin in the YAC128 mouse model of Huntington disease. *Hum. Mol. Genet.* **14,** 3823–3835
44. Wheeler, V. C., White, J. K., Gutekunst, C. A., Vrbanac, V., Weaver, M., Li, X. J., Li, S. H., Yi, H., Vonsattel, J. P., Gusella, J. F., Hersch, S., Auerbach, W., Joyner, A. L., and MacDonald, M. E. (2000) Long glutamine tracts cause nuclear localization of a novel form of huntingtin in medium spiny striatal neurons in HdhQ92 and HdhQ111 knock-in mice. *Hum. Mol. Genet.* **9,** 503–513
45. Menalled, L. B., Sison, J. D., Dragatsis, I., Zeitlin, S., and Chesselet, M. F. (2003) Time course of early motor and neuropathological anomalies in a knock-in mouse model of Huntington's disease with 140 CAG repeats. *J. Comp. Neurol.* **465,** 11–26
46. Legleiter, J., Mitchell, E., Lotz, G. P., Sapp, E., Ng, C., DiFiglia, M., Thompson, L. M., and Muchowski, P. J. (2010) Mutant huntingtin fragments form oligomers in a polyglutamine length-dependent manner *in vitro* and *in vivo*. *J. Biol. Chem.* **285,** 14777–14790
47. Colby, D. W., Cassady, J. P., Lin, G. C., Ingram, V. M., and Wittrup, K. D. (2006) Stochastic kinetics of intracellular huntingtin aggregate formation. *Nat. Chem. Biol.* **2,** 319–323
48. Colby, D. W., Chu, Y., Cassady, J. P., Duennwald, M., Zazulak, H., Webster, J. M., Messer, A., Lindquist, S., Ingram, V. M., and Wittrup, K. D. (2004) Potent inhibition of huntingtin aggregation and cytotoxicity by a disulfide bond-free single-domain intracellular antibody. *Proc. Natl. Acad. Sci. U.S.A.* **101,** 17616–17621